BIOENERGY AND BIOFUELS

Comparative global metabolite profiling of xylose-fermenting *Saccharomyces cerevisiae* SR8 and *Scheffersomyces stipitis*

Minhye Shin[1] · Jeong-won Kim[2] · Suji Ye[2] · Sooah Kim[1] · Deokyeol Jeong[2] · Do Yup Lee[3] · Jong Nam Kim[4] · Yong-Su Jin[5] · Kyoung Heon Kim[1] · Soo Rin Kim[2]

Abstract

Bioconversion of lignocellulosic biomass into ethanol requires efficient xylose fermentation. Previously, we developed an engineered *Saccharomyces cerevisiae* strain, named SR8, through rational and inverse metabolic engineering strategies, thereby improving its xylose fermentation and ethanol production. However, its fermentation characteristics have not yet been fully evaluated. In this study, we investigated the xylose fermentation and metabolic profiles for ethanol production in the SR8 strain compared with native *Scheffersomyces stipitis*. The SR8 strain showed a higher maximum ethanol titer and xylose consumption rate when cultured with a high concentration of xylose, mixed sugars, and under anaerobic conditions than *Sch. stipitis*. However, its ethanol productivity was less on 40 g/L xylose as the sole carbon source, mainly due to the formation of xylitol and glycerol. Global metabolite profiling indicated different intracellular production rates of xylulose and glycerol-3-phosphate in the two strains. In addition, compared with *Sch. stipitis*, SR8 had increased abundances of metabolites from sugar metabolism and decreased abundances of metabolites from energy metabolism and free fatty acids. These results provide insights into how to control and balance redox cofactors for the production of fuels and chemicals from xylose by the engineered *S. cerevisiae*.

Keywords *Saccharomyces cerevisiae* · *Scheffersomyces stipitis* · GC-TOF/MS · Metabolomics · Xylose fermentation

Introduction

Lignocellulosic ethanol production is a renewable liquid fuel alternative closest to commercialization, while xylose is the second most abundant sugar in the hydrolysates of lignocellulosic-based feedstocks. However, it is challenging for microorganisms to ferment xylose. *Saccharomyces cerevisiae* is one of the most common strains that produce

✉ Soo Rin Kim
  soorinkim@knu.ac.kr

1 Department of Biotechnology, Graduate School, Korea University, Seoul, Korea

2 School of Food Science and Biotechnology, Kyungpook National University, Daegu, Korea

3 Department of Bio and Fermentation Convergence Technology, BK21 PLUS Program, Kookmin University, Seoul, Korea

4 Department of Food Science and Nutrition, Dongseo University, Busan, Korea

5 Department of Food Science and Human Nutrition, the University of Illinois at Urbana-Champaign, Urbana, IL, USA

ethanol from feedstocks by fermenting hexoses or disaccharides. Nevertheless, it has a limited range of pentose sugar fermentation (Kwak and Jin 2017). Accordingly, substantial research effort has been put into enabling *S. cerevisiae* to utilize xylose (Øverland and Skrede 2017).

Scheffersomyces stipitis is one of the most studied yeasts regarding its biochemistry of xylose assimilation and xylose conversion into ethanol (Acevedo et al. 2017). For the heterologous expression of xylose-utilizing genes in eukaryotic host systems, those from *Sch. stipitis* have been more widely introduced than for any other eukaryotic xylose pathway (du Preez and Prior 1985; Jeffries and Van Vleet 2009). However, *S. cerevisiae* is a robust organism with a high tolerance to inhibitors such as furfural and methyl furfural as well as to ethanol products, whereas *Sch. stipitis* shows less tolerance (Hahn-Hägerdal et al. 2007). In addition, the culture conditions associated with high ethanol production are in a narrow range of oxygen concentration, so effective control of the oxygen supply is required (Silva et al. 2010).

S. cerevisiae has advantages over the innate xylose-utilizing microorganisms regarding robustness against various stresses, such as low pH, high osmotic pressure, and high

alcohol concentration (Hong and Nielsen 2012; Kwak and Jin 2017). For this reason, to enable *S. cerevisiae* to assimilate xylose, the most common strategy to introduce the fungal pathway from *Sch. stipitis* consists of the xylose reductase (XR, encoded by the *XYL1* gene) and xylitol dehydrogenase (XDH, encoded by the *XYL2* gene) pathways (Kötter et al. 1990; Tantirungkij et al. 1993; Walfridsson et al. 1995; Ho et al. 1998; Toivari et al. 2001). XR catalyzes the reduction of xylose to xylitol, then XDH subsequently oxidizes xylitol to xylulose. However, XR uses both NADH and NADPH, while XDH favors using NAD$^+$ only. This redox imbalance leads to xylitol accumulation and low ethanol yield in *S. cerevisiae*, which is the main problem to be resolved.

Recently, we have developed an engineered *S. cerevisiae* strain, named SR8, through rational and inverse metabolite engineering strategies (Kim et al. 2013). First, the SR8 strain possesses an optimized heterologous xylose-assimilating pathway by altering the copy numbers of *XYL1*, *XYL2*, and *XYL3*. Second, the SR8 strain is a product of evolutionary engineering which has overcome xylose toxicity resulting in a long lag time through serial subcultures on xylose. Mutations have evolved in *PHO13* as a loss-of-function which may block a futile cycle with xylulokinase overexpression associated with shorter lag time and improved xylose-fermenting capabilities compared with the parental strain. Third, the SR8 strain has a deletion in the *ALD6* gene encoding acetaldehyde dehydrogenase which prevents acetate accumulation. This simple set of genetic perturbations has allowed the co-fermentation of glucose and xylose at various concentrations. However, its fermentation profile in anaerobic conditions and at very high xylose concentrations has not yet been studied.

A global system-based approach to investigate changes in small-molecule metabolite profiles has become an important tool to understand phenotypes and fermentation outcomes in biological processes. In the present study, we investigated and compared xylose fermentation profiles for ethanol production in the engineered *S. cerevisiae* SR8 and native *Sch. stipitis*. Using metabolomic approaches, we examined metabolic changes elicited in the two strains associated with fermentation phenotypes under micro-aerobic and anaerobic conditions. These results could be further utilized to engineer microorganisms that can overcome by-product formation during xylose fermentation and ethanol production.

Materials and methods

Culture conditions and flask fermentation experiments

Yeast cells (*S. cerevisiae* SR8 and *Sch. stipitis* CBS6054) were precultured in 5 mL of YP medium (10 g/L yeast extract and 20 g/L peptone) containing 20 g/L glucose (YPD) for 24 h at 250 rpm. Cells were harvested by centrifugation at 15,000 rpm for 1 min. The adjusted OD$_{600}$ 1.0 (OD$_{600}$ 1.0 = 3.5×10^7 cells/mL) of initial cell concentration was added to 20 mL of YPX 40 (40 g/L xylose), YPX 80 (80 g/L xylose), YPX 120 (120 g/L xylose), and YPDX 70, 40 (70 g/L glucose and 40 g/L xylose) in a 100-mL Erlenmeyer flask at 30 °C and agitated at 80 rpm. Anaerobic cultivation was performed at 30 °C in a 100-mL serum bottle with agitation at 130 rpm. All experiments were performed in triplicate.

Intracellular metabolite extraction

Metabolite extraction was conducted according to the method described by Jung et al. (Jung et al. 2017). Briefly, 5 mL of cell culture at the mid-exponential growth phase was quenched by quick injection into 25 mL of 60% (*v/v*) cold methanol (HEPES, 10 mM; pH 7.1) at − 40 °C. The cells were centrifuged at 4000 rpm (3134×*g*) for 10 min at − 20 °C and the supernatant was removed thoroughly. Subsequently, 5 mL of 75% (*v/v*) boiling ethanol (HEPES, 10 mM; pH 7.1) was added to the quenched cell pellet. The mixture was vortexed for 30 s, incubated for 5 min at 80 °C, and then immediately cooled in an ice bath for 5 min. The cell residues were separated from the extract by centrifugation at 4000 rpm (3134×*g*) for 10 min at 4 °C. The supernatant (0.2 mL) was vacuum-dried for 6 h using a speed vacuum concentrator.

Metabolite analysis using gas chromatography/mass spectrometry (GC/MS)

Prior to the GC/MS analysis, the vacuum-dried samples were derivatized by methoxyamination and trimethylsilylation. For methoxyamination, 40 μL of methoxyamine hydrochloride in pyridine (40 mg/mL; Sigma-Aldrich, St. Louis, MO) was added to the samples and incubated for 90 min at 30 °C. For trimethylsilylation, 40 μL of *N*-methyl-*N*-(trimethylsilyl)trifluoroacetamide (Sigma-Aldrich, St. Louis, MO, USA) was added to the samples and incubated for 30 min at 37 °C.

The GC/MS analysis was conducted using an Agilent 6890 GC equipped with an Agilent 5973 mass selective detector (Agilent, Santa Clara, CA, USA). A 1-μL aliquot of derivatized samples was injected into the GC in splitless mode and separated on an RTX-5Sil MS column (30 m × 0.25 mm, 0.25-μm film thickness; Restek, Bellefonte, PA). The initial oven temperature was set at 50 °C for 1 min, then ramped at 20 °C/min to a final temperature of 330 °C and held for 2 min. Helium was used as the carrier gas at a constant flow rate of 1.5 mL/min. The temperatures of the ion source and transfer line were set at 250 °C and 280 °C, respectively. An electron impact of 70 eV was used for the ionization. The mass
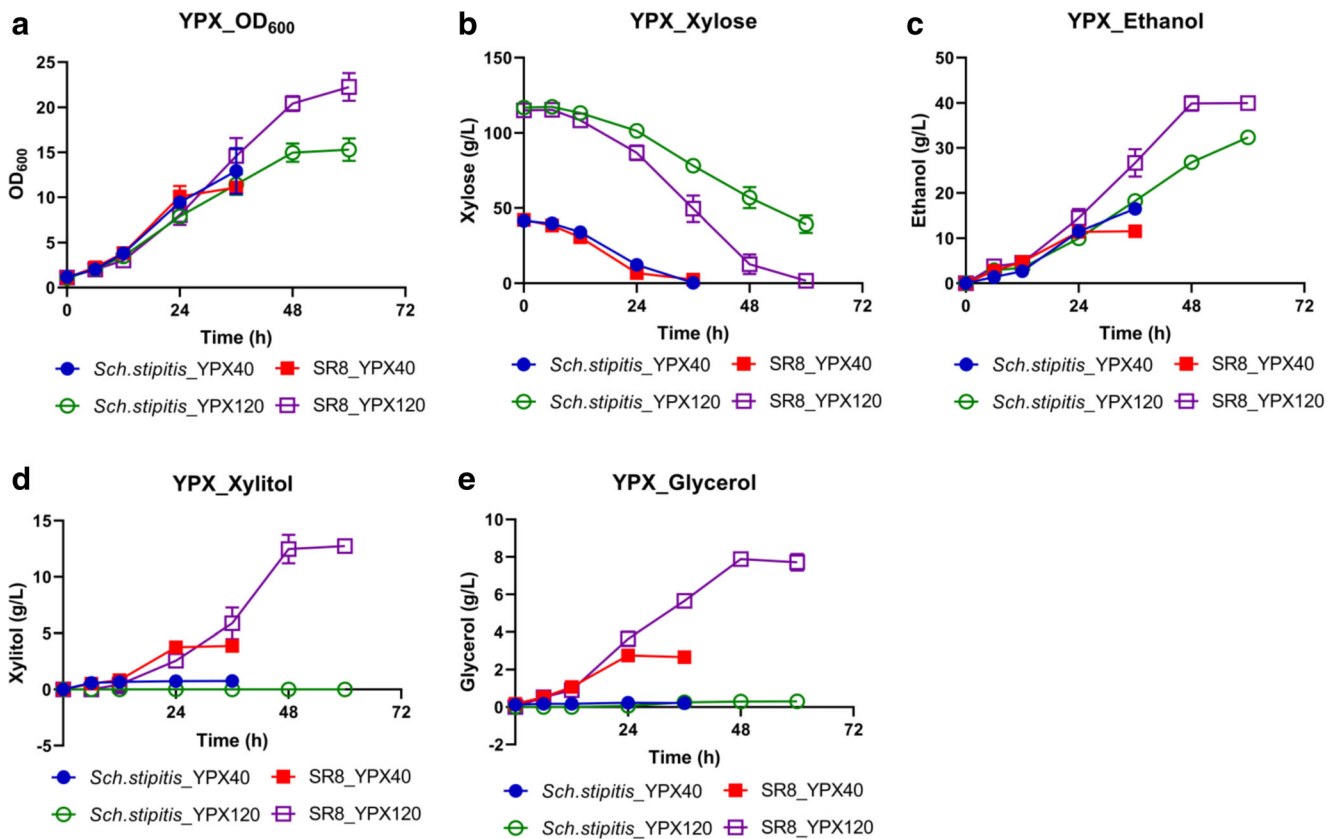
Fig. 1 **a**–**e** Fermentation profiles of *Sch. stipitis* CBS 6054 and *S. cerevisiae* SR8 in YP medium containing 40 g/L or 120 g/L xylose under micro-aerobic conditions at 30 °C. The initial cell density was OD_{600} = 1.0. All of the experiments were performed in triplicate. Blue-filled circle, *Sch. stipitis* grown with 40 g/L xylose; red-filled square, SR8 grown with 40 g/L xylose; green circle, *Sch. stipitis* grown with 120 g/L xylose; and violet square, SR8 grown with 120 g/L xylose

selective detector was operated in scan mode with a mass range of 50–800 *m/z*.

High-performance liquid chromatography (HPLC) analysis

The concentrations of xylose, xylitol, glycerol, acetate, and ethanol in the culture were determined via HPLC (Agilent Technologies 1260 Series, Santa Clara, CA, USA) equipped with a refractive index detector using a Rezex ROA-Organic Acid H^+ (8%) column (Phenomenex, Inc., Torrance, CA, USA). The column was eluted with 0.005 N H_2SO_4 at a flow rate of 0.6 mL/min at 50 °C.

Statistical analysis

The metabolites were evaluated with a principal component analysis (PCA) using STATISTICA software (Version 7.0, Stat Soft, Tulsa, OK, USA). The significance ($p < 0.05$) of the presented based on a *t* test was determined using SPSS software (Version 23.0, SPSS, Inc., Chicago, IL, USA).

Data availability

The datasets supporting the conclusions of this article are included within it.

Results

The engineered *S. cerevisiae* SR8 shows faster xylose fermentation than native *Sch. stipitis* under a high concentration of xylose

The *S. cerevisiae* SR8 strain expressing *XYL1*, *XYL2*, and *XYL3* has been evolutionarily engineered to overcome growth inhibition at 40 g/L xylose (Kim et al. 2013; Kim et al. 2015). To characterize the xylose fermentation performance of the SR8 strain, we compared native *Sch. stipitis* and the SR8 strains micro-aerobically grown with 40 g/L or 120 g/L xylose concentrations. Under 40 g/L xylose, the specific growth and xylose consumption rates were similar between the two strains (Fig. 1 and Table 1). However, due to the formation of by-

Table 1 Fermentation profiles of *Sch. stipitis* CBS 6054 and *S. cerevisiae* SR8 under various sugar and oxygen conditions

	Micro-aerobic conditions						Anaerobic conditions	
	40 g/L xylose (at 36 h)		120 g/L xylose (at 60 h)		40 g/L xylose and 70 g/L glucose (at 60 h)		40 g/L xylose (at 96 h)	
	Sch. stipitis	SR8	*Sch. stipitis*	SR8	*Sch. stipitis*	SR8	*Sch. stipitis*	SR8
Ethanol (g/L)	16.50 ± 0.21	$11.55 \pm 1.11^{*}$	32.37 ± 0.99	$39.98 \pm 1.09^{*}$	30.07 ± 0.62	$39.54 \pm 0.11^{*}$	6.14 ± 0.08	$10.94 \pm 0.25^{*}$
μ	$0.16 \pm 0.01^{2)}$	0.16 ± 0.02	0.13 ± 0.01	$0.17 \pm 0.01^{*}$	0.18 ± 0.00	0.17 ± 0.01	0.05 ± 0.00	$0.07 \pm 0.00^{*}$
r_{xylose}	1.15 ± 0.01	1.10 ± 0.03	1.29 ± 0.09	$1.89 \pm 0.02^{*}$	1.44 ± 0.07	$1.78 \pm 0.01^{*}$	0.13 ± 0.01	$0.42 \pm 0.00^{*}$
$Y_{xylitol}$	0.02 ± 0.00	$0.10 \pm 0.00^{*}$	0.00 ± 0.00	$0.11 \pm 0.00^{*}$	0.05 ± 0.00	$0.03 \pm 0.00^{*}$	0.08 ± 0.01	$0.32 \pm 0.01^{*}$
$Y_{glycerol}$	0.01 ± 0.00	$0.07 \pm 0.00^{*}$	0.00 ± 0.00	$0.07 \pm 0.00^{*}$	0.01 ± 0.00	$0.04 \pm 0.00^{*}$	0.03 ± 0.00	$0.08 \pm 0.00^{*}$
$Y_{ethanol}$	0.40 ± 0.00	$0.29 \pm 0.03^{*}$	0.42 ± 0.02	$0.35 \pm 0.01^{*}$	0.35 ± 0.01	$0.37 \pm 0.00^{*}$	0.48 ± 0.02	$0.27 \pm 0.01^{*}$

Parameters: μ, growth rate (ΔOD_{600}/h); r_{xylose}, xylose consumption rate (g/L/h); $Y_{xylitol}$, xylitol yield (g/g consumed sugars); $Y_{glycerol}$, glycerol yield (g/g consumed sugars); and $Y_{ethanol}$, ethanol yield (g/g consumed sugars). All of the rate parameters were calculated when more than 90% of the xylose was consumed under each set of conditions

[1] Fermentations were conducted in YP medium at 30 °C and the initial cell density was $OD_{600} = 1.0$

[2] Values are the mean ± standard deviations from three biological replicates

[*] Significant difference ($p < 0.05$) between the *Sch. stipitis* and SR8 strains

products (xylitol and glycerol), the ethanol yield and titer were lower in the SR8 strain.

When cultured in 120 g/L xylose as the sole carbon source, the SR8 strain exhibited faster xylose fermentation and cellular growth rate than native *Sch. stipitis* (Fig. 1 and Table 1). The SR8 strain consumed almost all of the xylose provided (98.6 ± 0.59%) and produced 40 g/L of ethanol within 60 h. However, similar to the lower xylose concentration condition (40 g/L xylose), the strain generated a considerable amount of xylitol and glycerol as by-products, while *Sch. stipitis* only produced trace amounts of these (12.7 ± 0.30 g/L and 7.71 ± 0.44 g/L, respectively).

Meanwhile, to elucidate the mechanisms underlying changes in the fermentation profile, the yields of biomass, ethanol, xylitol, and glycerol were compared from various concentrations of xylose (40, 80, and 120 g/L; Fig. 2). Both strains showed similar biomass production per gram of xylose consumed (0.12~0.19 g cells/g xylose). However, the average ethanol yields of SR8 (0.32 ± 0.031 g/g xylose) and *Sch. stipitis* (0.40 ± 0.028 g/g xylose) were significantly different. Moreover, the high yields of xylitol (0.10 ± 0.0081 g/g) and glycerol (0.070 ± 0.0065 g/g) of the SR8 strain were noticed at all xylose concentrations, which were one order of magnitude lower in *Sch. stipitis* (0.010 ± 0.0099 and 0.003 ± 0.0023 g/g, respectively). The calculated fermentation product ratio (ethanol:xylitol:glycerol) of the engineered SR8 strain was 65:20:14 whereas that of *Sch. stipitis* was 97:2:1, with carbon recovery values of 79.3% and 79.5%, respectively. The results
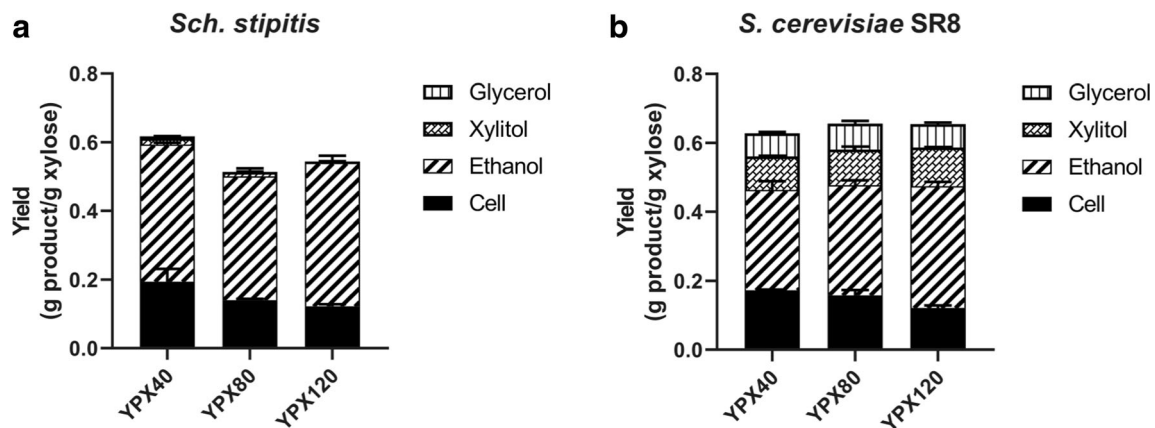
Fig. 2 Product yields of *Sch. stipitis* CBS 6054 (**a**) and *S. cerevisiae* SR8 (**b**) in YP medium containing 40 g/L, 80 g/L, or 120 g/L xylose under micro-aerobic conditions at 30 °C. The initial cell density was $OD_{600} = 1.0$. All of the experiments were performed in triplicate
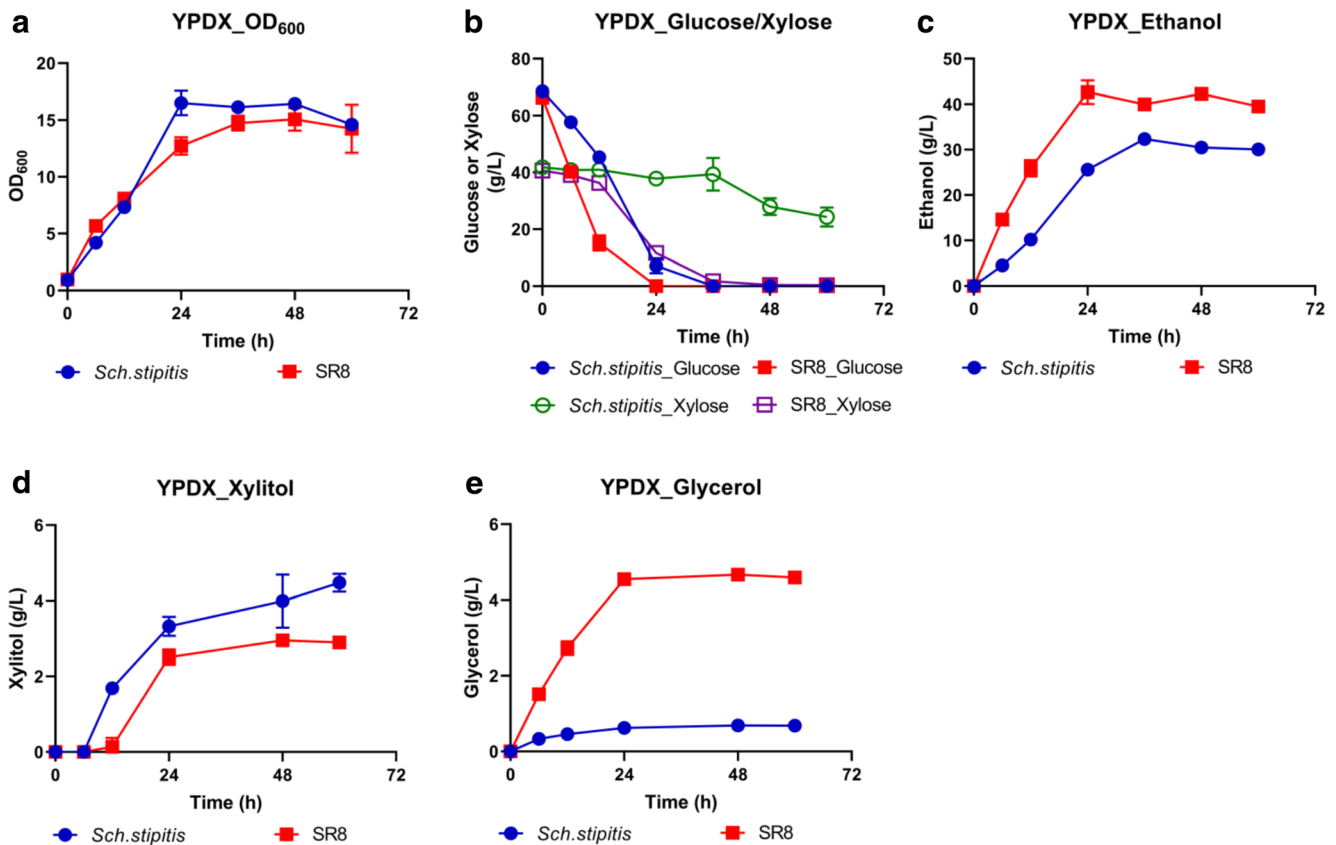
Fig. 3 a–e Fermentation profiles of *Sch. stipitis* CBS 6054 and *S. cerevisiae* SR8 in YP medium containing 70 g/L glucose and 40 g/L xylose under micro-aerobic conditions at 30 °C. The initial cell density was $OD_{600} = 1.0$. All of the experiments were performed in triplicate. Blue-filled circle, *Sch. stipitis*; red-filled square, SR8

suggest that the engineered SR8 strain and *Sch. stipitis* have completely different product partitioning patterns regardless of the external concentration of xylose.

The engineered *S. cerevisiae* SR8 shows higher ethanol production than native *Sch. stipitis* under the mixed sugar condition

Fermentation differences between the SR8 and *Sch. stipitis* strains were studied when cultured in a mixture of glucose (70 g/L) and xylose (40 g/L), presenting general sugar compositions of cellulosic biomass. Both strains favored consuming the glucose, then subsequently utilized the xylose after consuming all of the glucose (Fig. 3b). The SR8 strain completely consumed 70 g/L of glucose and 40 g/L of xylose within 24 and 48 h, respectively. Meanwhile, the *Sch. stipitis* strain consumed the glucose within 48 h, but hardly utilized the xylose (consuming only 44%). The SR8 strain produced ethanol from both glucose and xylose, resulting in 39.54 g/L of maximum ethanol titer for 60 h culture. However, *Sch. stipitis* mainly produced ethanol from glucose fermentation, and there was no additional ethanol production after 40 h when using xylose as the carbon source (Fig. 3c).

Interestingly, *Sch. stipitis* produced a higher concentration of xylitol (4.5 g/L) from the mixed sugar composition compared with the other conditions even higher than the SR8 strain.

Anaerobic conditions provide an advantage on xylose consumption and ethanol production to the engineered *S. cerevisiae* SR8

Xylose-fermenting yeasts are able to ferment xylose efficiently when the oxygen flow is tightly regulated (Veras et al. 2017). A high oxygen level leads to aerobic growth and low ethanol yield, whereas limited oxygen, like in anaerobic conditions, slows the fermentation rate, increases xylitol accumulation, and causes poor ethanol productivity (Hou 2012). To test the effects of anaerobic conditions on the ethanol production in the SR8 and *Sch. stipitis* strains, their fermentation profiles with a xylose medium (40 g/L) were compared. During the anaerobic fermenting, the SR8 strain gradually grew up to 5 g/L of cell biomass and consumed approximately 95.5% of the xylose within 96 h (Fig. 4). At the end of the fermentation, the SR8 strain generated 10.94 g/L of ethanol and an even higher concentration of xylitol (13.09 g/L).
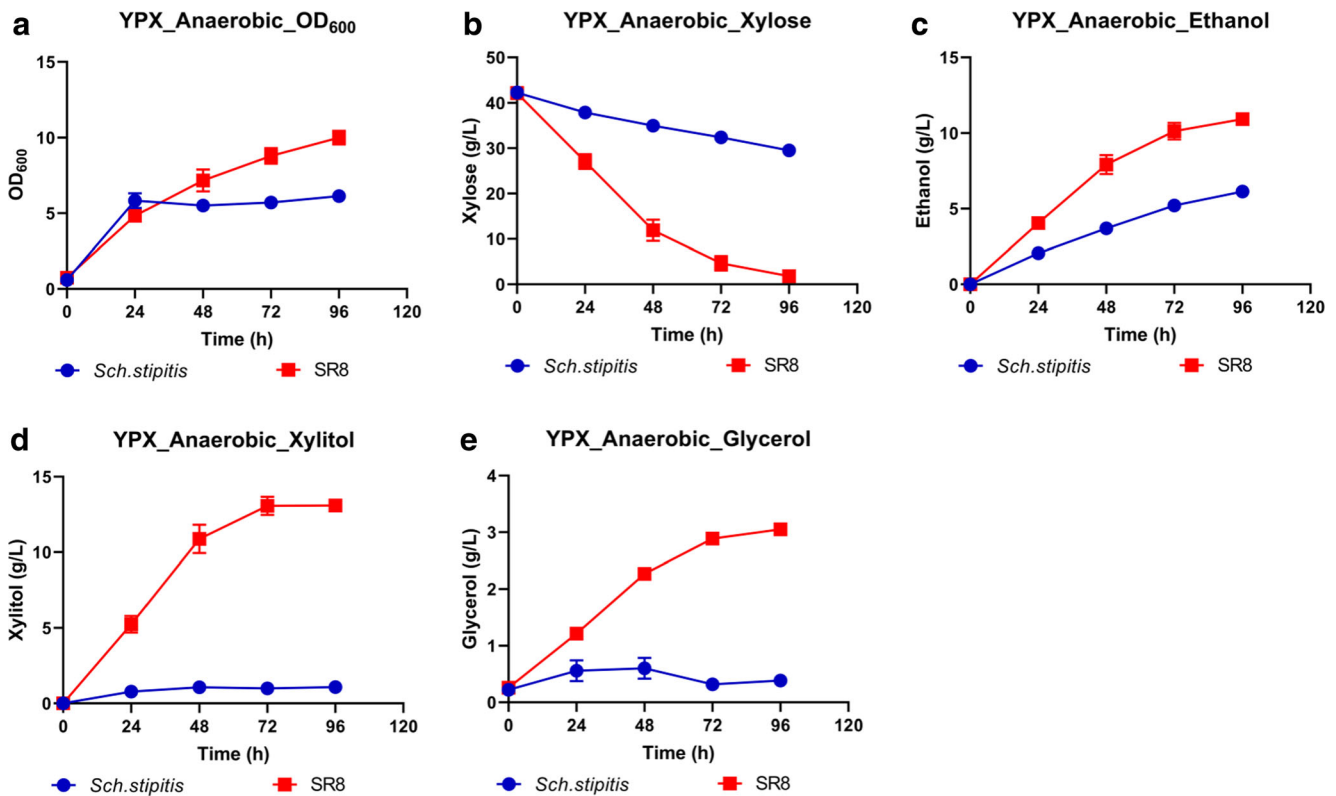
Fig. 4 **a**–**e** Fermentation profiles of *Sch. stipitis* CBS 6054 and *S. cerevisiae* SR8 in YP medium containing 40 g/L xylose under anaerobic conditions at 30 °C. The initial cell density was $OD_{600} = 1.0$. All of the experiments were performed in triplicate. Blue-filled circle, *Sch. stipitis*; red-filled square, SR8

Meanwhile, the *Sch. stipitis* strain only grew up to 3 g/L of cell biomass and hardly fermented the xylose.

Global metabolite profiling separates the different metabolic phenotypes of SR8 and *Sch. stipitis* grown with xylose as the carbon source

From the characterization of the various fermentation profiles of the two strains, we found that the SR8 strain always displayed a higher maximum ethanol titer and xylose consumption rate compared with the native *Sch. stipitis* strain, except when cultivated with 40 g/L xylose as the sole carbon source. The decrease in ethanol productivity from xylose metabolism mostly resulted from the unwanted production of xylitol and glycerol. To investigate distinct features in the metabolic physiology of the engineered yeast during xylose fermentation, a global metabolomic analysis based on GC-TOF/MS was conducted.

Seventy-eight intracellular metabolites, including organic acids, amino acids, sugar alcohols, and glycolysis intermediate metabolites, were detected in the cells micro-aerobically (oxygen-limited) or anaerobically grown with 40 g/L xylose at the mid-exponential phase. All detected metabolites were statistically evaluated via PCA. Both strains under different conditions were clearly separated in score plots, indicating that the

two strains have distinct features in xylose metabolism (Fig. 5a and b).

To find the specific metabolic pathways which are differently regulated in the two strains, we compared the fold-changes of intracellular metabolites from the two strains grown micro-aerobically (Figs. 5 and 6a) or anaerobically (Figs. 5 and 6b). Eight metabolites (mannose-6-phosphate, arginine, xylobiose, inosine, adenine, galactinol, fructose-1,6-bisphosphate, and trehalose-6-phosphate) increased and eight metabolites (xylulose, glycerol-3-phosphate, tetradecanoic acid, hexadecanoic acid, octadecanoic acid, fumaric acid, serine, and uracil) decreased in the SR8 strain compared with native *Sch. stipitis* under both micro-aerobic and anaerobic conditions. These metabolites were indicative of prominent features in the SR8 strain.

We further analyzed fold-changes in the intracellular metabolites from each strain grown micro-aerobically versus anaerobically (Figs. 5 and 6). Ten metabolites (pyruvic acid, ornithine-1,5-lactam, valine, aspartic acid, norleucine, glycine, lysine, furan-2-carboxylic acid, asparagine, and glycylproline) increased and five metabolites (pyridine, adenosine, propargyl alcohol, galactinol, and mannitol) decreased in the cells from both strains when grown micro-aerobically compared with anaerobically grown ones. These metabolites show the general metabolic changes between the microbial cells
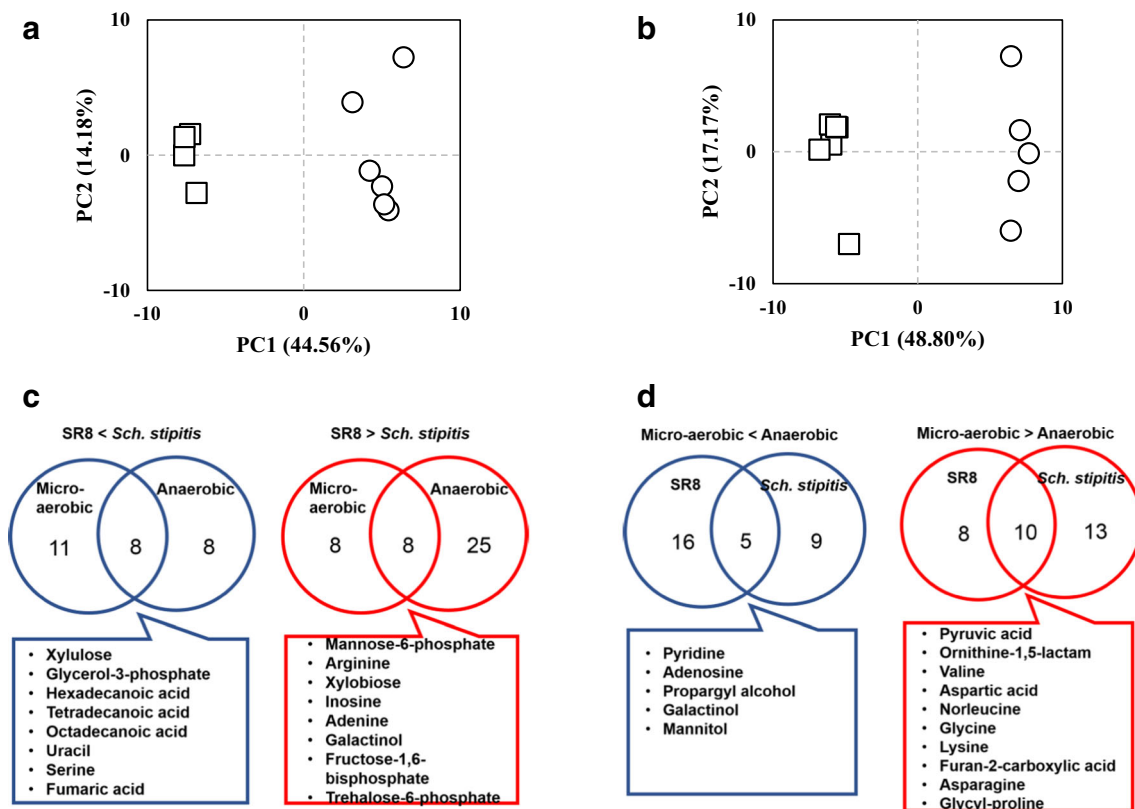
Fig. 5 Comparison of the intracellular metabolite profiles of SR8 and *Sch. stipitis* grown in YP medium containing 40 g/L xylose under micro-aerobic and anaerobic conditions. Intracellular metabolites were detected by GC/TOF-MS and all the relative abundance was evaluated. Score plots between SR8 (white square) and *Sch. stipitis* (white circle) grown under micro-aerobic (**a**) and anaerobic culture (**b**) conditions. Metabolites that increased in *Sch. stipitis* compared with SR8 under

both micro-aerobic and anaerobic conditions (the boxed metabolites that were more highly detected in *Sch. stipitis* than in SR8 regardless of the culture conditions) (**c**) and metabolites that increased in SR8 compared with *Sch. stipitis* under micro-aerobic and anaerobic conditions (the boxed metabolites that were more highly detected in SR8 than *Sch. stipitis* regardless of the culture conditions) (**d**)

from the micro-aerobic and anaerobic environments. With respect to the differences in the strains, the micro-aerobic conditions caused SR8 to produce more xylulose than the anaerobic conditions, while xylulose production was higher in the anaerobically grown *Sch. stipitis* cells than the micro-aerobically grown ones.

Xylulose and glycerol-3-phosphate are key determinants for xylitol and glycerol accumulation

From the global metabolome, we selected five specific intracellular metabolites (xylitol, xylulose, fructose-1,6-bisphosphate, glycerol-3-phosphate, and glycerol) which are the main intermediates in xylose fermentation (Fig. 7). Under the micro-aerobic conditions, we detected significantly more xylitol in the SR8 strain than *Sch. stipitis* ($p < 0.05$, Fig. 7a). Xylulose, which is further oxidized from xylitol by xylitol dehydrogenase, decreased further in SR8 than *Sch. stipitis*. Meanwhile, fructose-1,6-bisphosphate was only detected in SR8 at the mid-exponential phase. Glycerol-3-phosphate,

which is converted from dihydroxyacetone phosphate by glycerol-3-phosphate dehydrogenase, significantly increased in *Sch. stipitis*. Unlike glycerol-3-phosphate, the glycerol concentration was higher in SR8 compared with *Sch. stipitis*, which suggests that xylitol accumulation could have resulted from an insufficient supply of NAD^+ followed by inefficient oxidation of xylitol to xylulose, and glycerol could have been overproduced to deplete glycerol-3-phosphate during the process of NAD^+ regeneration by glycerol-3-phosphate dehydrogenase to provide NAD^+ for xylitol oxidation (Rho and Choi 2018).

The anaerobic culture conditions resulted in a similar intracellular metabolite pattern in the xylose-fermenting pathway compared with the pattern in the micro-aerobically grown culture, except for xylitol (Fig. 7). However, the individual concentrations of each metabolite were different between the two culture conditions. While xylitol, xylulose, and glycerol-3-phosphate increased under the anaerobic conditions, fructose-1,6-bisphosphate decreased, indicating deficient substrate-level phosphorylation from glycolysis and an

Fig. 6 Intracellular metabolite fold-changes in SR8 and *Sch. stipitis* grown in YP medium containing 40 g/L xylose under micro-aerobic and anaerobic conditions. Intracellular metabolites were detected using GC/TOF-MS and fold-changes were converted to a log 2 scale. Comparisons were conducted between SR8 and *Sch. stipitis* under micro-aerobic (**a**) and anaerobic (**b**) conditions, and between micro-aerobic and anaerobic conditions in SR8 (**c**) and *Sch. stipitis* (**d**)
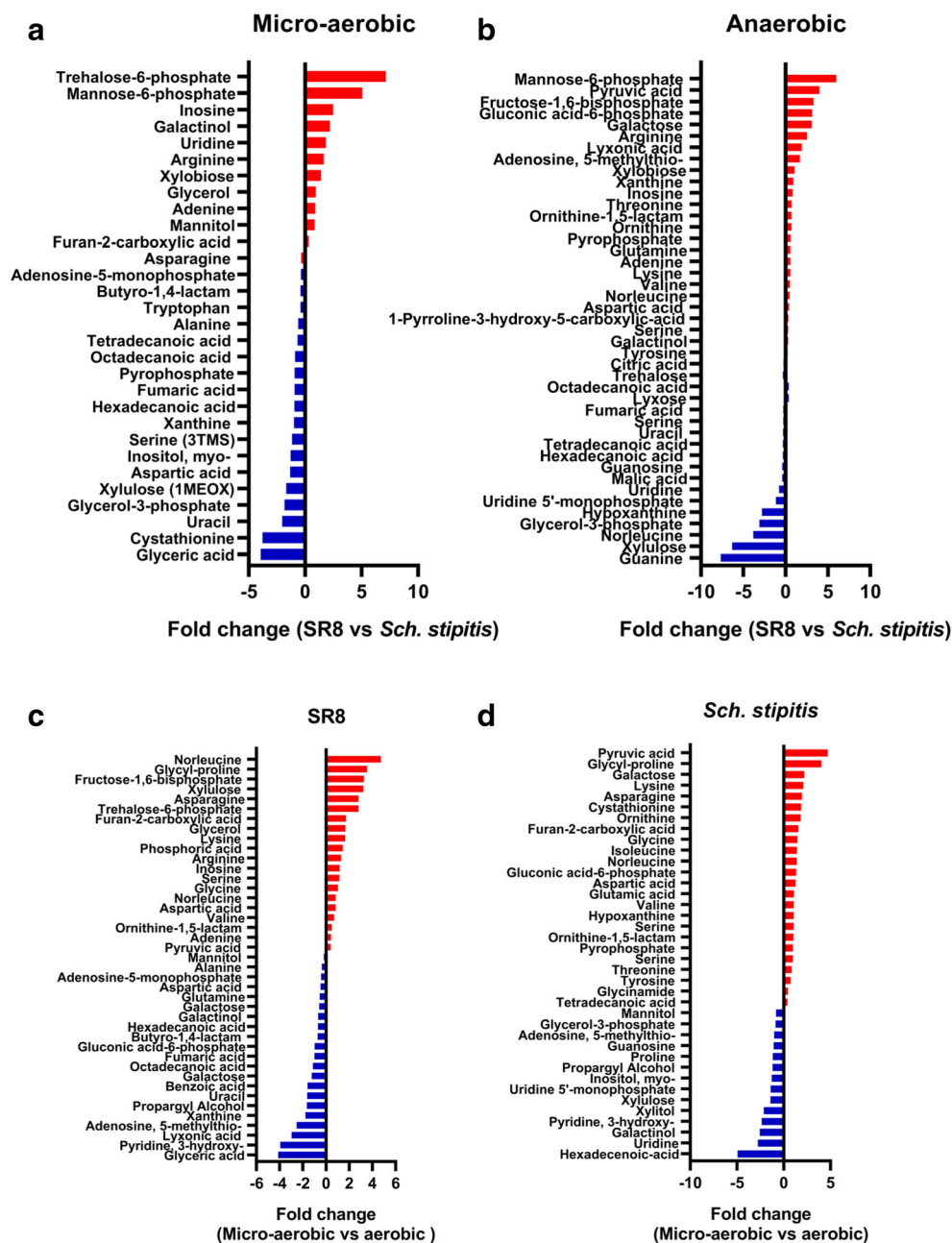

imbalance in the redox cofactors under the oxygen-restricted conditions.

Global metabolite profiling reveals distinct changes in central carbon and fatty acid metabolism for xylose fermentation

In addition to changes in the specific xylose fermentative pathway, our global metabolite profiling also showed that several metabolic pathways, including central carbon and fatty acid metabolism, were regulated differently in the SR8 and *Sch. stipitis* strains. In the central carbon metabolism, we detected increases in mannose-6-phosphate, mannitol, and trehalose-6-phosphate and decreases in fumaric acid, malic acid, alanine, and serine in the SR8 strain compared with native *Sch. stipitis* under the micro-aerobically grown culture conditions (Fig. 8). Interestingly, the concentration of free fatty acids was much higher in *Sch. stipitis* than SR8 (Fig. 9). The anaerobic conditions resulted in similar patterns of change in the metabolites, albeit not significantly different ones, except for mannose-6-phosphate and trehalose-6-phosphate (Figs. 8 and 9).
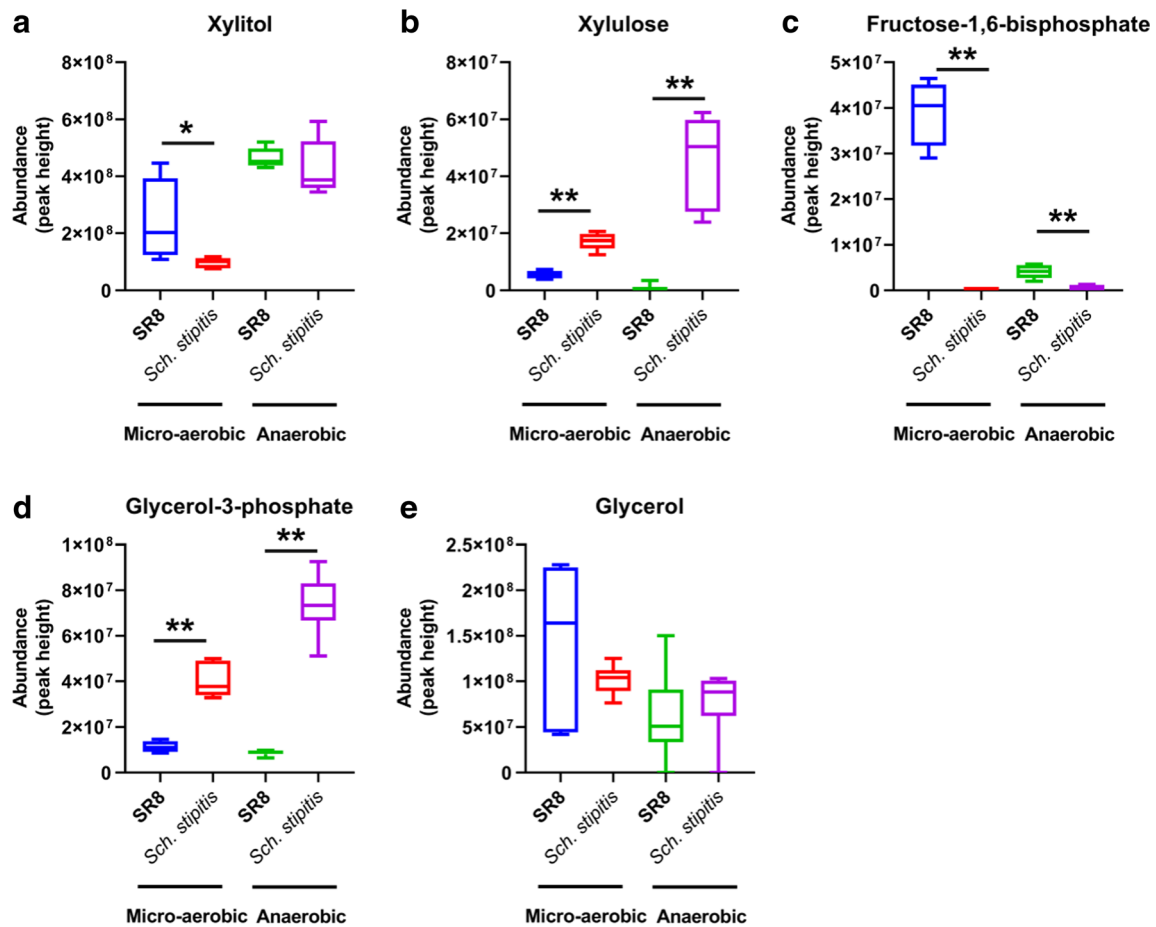
Fig. 7 a–e Abundances of the main intermediate metabolites in SR8 and *Sch. stipitis* grown in YP medium containing 40 g/L xylose under micro-aerobic and anaerobic conditions. The box extending from the 25th to the 75th percentile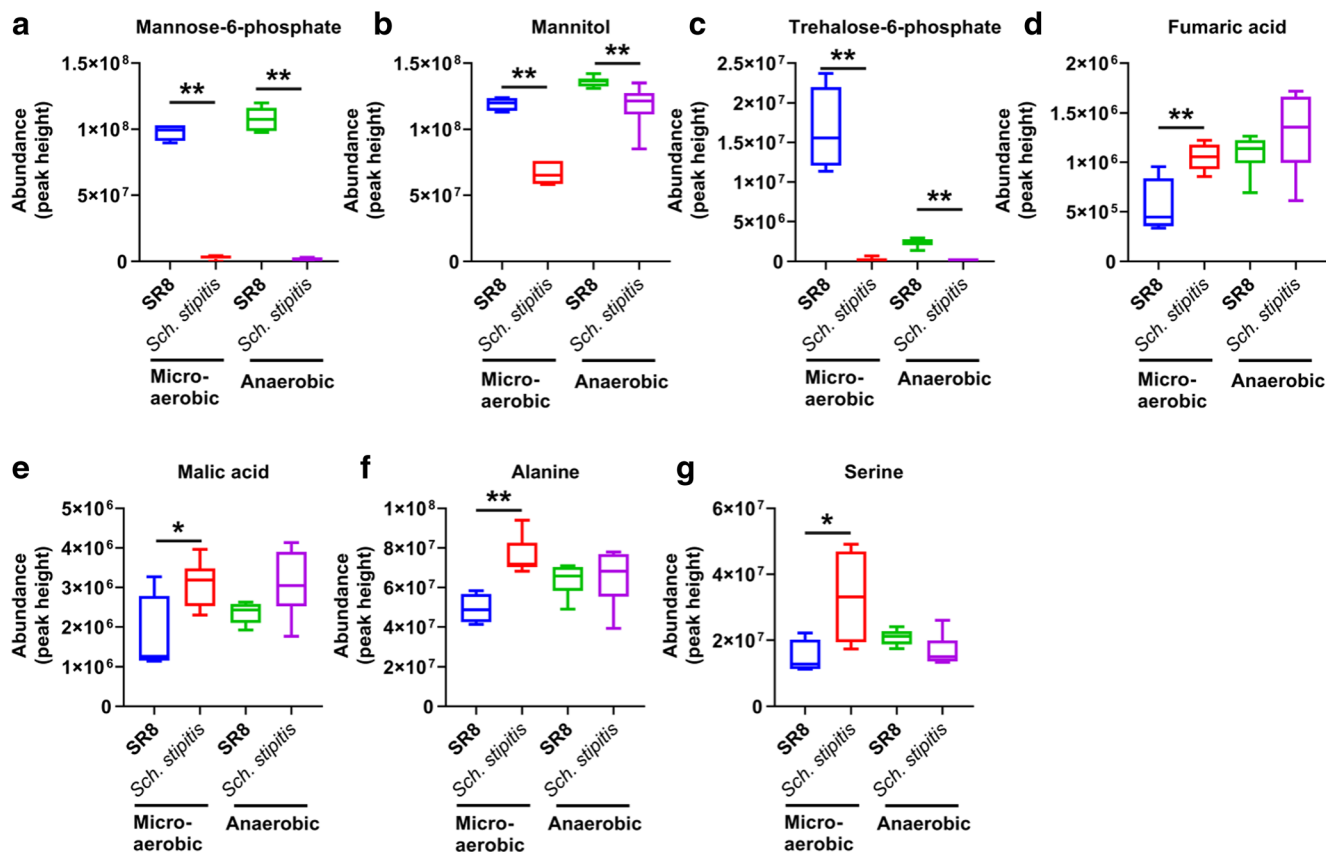s and the line in the middle of the box are plotted at the median. The whiskers go down and up to the minimum and maximum values, respectively. *p* values were calculated via a *t* test: * and ** denote significant differences at $p < 0.05$ and $p < 0.01$, respectively

Discussion

Sch. stipitis is widely known as an innate xylose-fermenting yeast strain. Genes encoding the xylose assimilation pathway in *Sch. stipitis* have been introduced into *S. cerevisiae* more often than from any other yeast strain. SR8 is an engineered *S. cerevisiae* strain heterologously expressing XR and XDH originating from *Sch. stipitis*. Utilizing rational and directed evolutionary engineering techniques, the strain has obtained powerful xylose fermentation capabilities. In this study, we compared the fermentation profiles of the SR8 and the *Sch. stipitis* strains under different culture conditions by varying carbon sources and oxygen-accessibility. The SR8 strain showed a higher maximum ethanol titer and xylose consumption rate when cultured on a high concentration of xylose (Fig. 1 and Table 1), mixed sugars (Fig. 3 and Table 1), and under anaerobic conditions (Fig. 4 and Table 1). However, its ethanol productivity was less than *Sch. stipitis* on 40 g/L xylose as the sole carbon source, mainly due to the formation of xylitol and glycerol (Fig. 1 and Table 1). Global metabolite profiling

indicated different intracellular production levels of xylulose and glycerol-3-phosphate in the two strains (Fig. 7). In addition, compared with *Sch. stipitis*, SR8 had increased abundances of metabolites of sugar metabolism (Fig. 8) and decreased abundances of metabolites of energy metabolism and free fatty acids (Figs. 8 and 9).

From the fermentation and metabolome profile analysis results (Figs. 2 and 7), we found that SR8 produces xylitol and glycerol as by-products, possibly resulting from the insufficient supply of NAD^+ (Zhang et al. 2012), but these products were not detected in *Sch. stipitis*, except for the mixed sugar composition. Recently, Hilliard et al. reported that XR in *Sch. stipitis* shifts its cofactor preference depending on the oxygen uptake rate (OUR) (Hilliard et al. 2018). As OUR decreases, the oxidation of NADH through oxidative phosphorylation becomes less necessary, and thus the availability of NADH increases. This shifts the redox cofactor specificity of XR to NADH, resulting in the decreased use of NADPH as well as decreased flux via the oxidative pentose phosphate pathway in *Sch. stipitis* on xylose (Hilliard et al. 2018). On the contrary, when oxygen
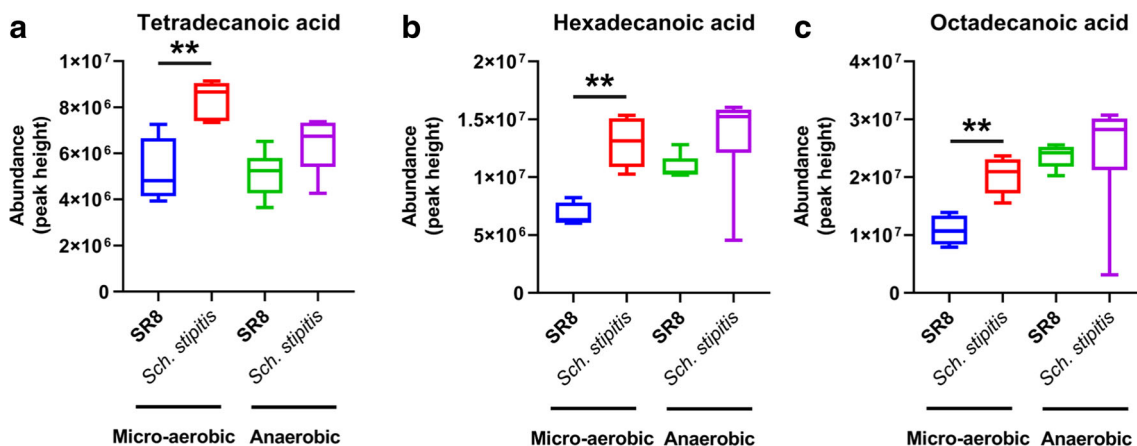
Fig. 8 a–g Abundances of the intermediate metabolites of central carbon metabolism in SR8 and *Sch. stipitis* grown in YP medium containing 40 g/L xylose under micro-aerobic and anaerobic conditions. The box extending from the 25th to the 75th percentiles and the line in the middle of the box are plotted at the median. The whiskers go down and up to the minimum and maximum values, respectively. *p* values were calculated via a *t* test: * and ** denote significant differences at $p < 0.05$ and $p < 0.01$, respectively

uptake is sufficient, NADH becomes less available because of NADH oxidation through oxidative phosphorylation. This shifts the redox cofactor specificity of XR to NADPH, resulting in increased flux via the pentose phosphate pathway as well as oxidative phosphorylation. Combined with our findings, we speculate that *Sch. stipitis* controls the redox cofactor balance on xylose fermentation more efficiently than *S. cerevisiae* by switching the cofactor preference of XR. Although the SR8 strain expresses XR and XDH originating from *Sch. stipitis*, its redox cofactor environment and control system could be

Fig. 9 a–c Abundances of free fatty acids of SR8 and *Sch. stipitis* grown in YP medium containing 40 g/L xylose under micro-aerobic and anaerobic conditions. The box extending from the 25th to the 75th percentiles and the line in the middle of the box are plotted at the median. The whiskers go down and up to the minimum and maximum values, respectively. *p* values were calculated via a *t* test: * and ** denote significant differences at $p < 0.05$ and $p < 0.01$, respectively.

different and less efficient. It is also noteworthy that with mixed sugars of glucose and xylose, *Sch. stipitis* can ferment both sugars through the concerted glycolytic and pentose phosphate pathways. During this process, an imbalance in redox cofactors occurs, resulting in deprivation of NAD^+ for the oxidation of xylitol and its subsequent accumulation.

Global metabolome profiling provides chemical fingerprints specifying unique or differential cellular processes. Using the technique, we compared the metabolic changes in the two strains, SR8 and *Sch. stipitis*, associated with the fermentation phenotypes under micro-aerobic and anaerobic conditions. The results clearly showed 1) increased abundances of metabolites from carbohydrate metabolism, 2) decreased abundances of metabolites from energy metabolism, and 3) decreased abundances of free fatty acids in SR8 compared with *Sch. stipitis*.

The Crabtree effect is a phenomenon described as the glucose-induced inhibition of cellular respiratory flux (Lemus et al. 2018). As a Crabtree-positive strain, *S. cerevisiae* produces ethanol under aerobic and high glucose conditions via strong glycolytic flux rather than producing biomass via the tricarboxylic acid (TCA) cycle. On the other hand, *Sch. stipitis* is a Crabtree-negative strain in which fermentation is regulated by a decrease in oxygen levels and is not dependent on the sugar concentration. SR8 showed higher abundances of fructose-6-phosphate derivatives (fructose-1,6-bisphosphate, mannose-6-phosphate, and mannitol) during xylose metabolism (40 g/L) under both micro-aerobic and anaerobic conditions (Figs. 7 and 8). High content of the fructose-1,6-bisphosphate, the phosphorylation product of fructose-6-phosphate by phosphofructokinase, is known as an important indicator of glycolytic hyperactivity (Peeters et al. 2017). Because the non-oxidative pentose phosphate pathway of xylose metabolism is connected to both upper and lower glycolytic pathways, the high abundance of fructose-1,6-bisphosphate in SR8 might indicate strong glycolytic activity during xylose metabolism as well. However, to support the regulatory role of fructose-1,6-bisphosphate during xylose metabolism in SR8, further evidence needs to be provided with time-course analysis of glycolytic intermediates as well as molecular level analysis of its mechanism of action. Meanwhile, mannose-6-phosphate and mannitol are generated from fructose-6-phosphate in a process catalyzed by phosphomannose isomerase and NADH-specific mannitol dehydrogenase, respectively. Therefore, there might be some interaction between the xylose metabolism lacking NAD^+ and the mannitol production yielding NAD^+.

Different from SR8, Crabtree-negative *Sch. stipitis* had higher abundances of fumaric acid and malic acid in the TCA cycle, suggesting more flux through the latter to acquire energy. In addition, this energy generation through the TCA cycle, ultimately followed by oxidative phosphorylation, makes more NAD^+ cofactor for the XR activity. Higher abundances of alanine and serine, derived from 3-phosphoglycerate and pyruvate,

respectively, in *Sch. stipitis* may be explained in line with the higher metabolite abundances in energy metabolism.

Meanwhile, the accumulation of sugar phosphates in SR8 can be explained by a loss-of-function mutation in the *PHO13* gene. In *E. coli*, haloacid dehalogenase–like phosphatases, where Pho13 belongs in the superfamily, exhibit substrate promiscuity with very wide and overlapping substrate ranges, including pentose and hexose phosphates (Kuznetsova et al. 2006; Kim et al. 2015). Currently, it is not clear whether eukaryotic Pho13 is closely related to bacterial orthologs or not. However, our results could provide more information on the role and substrate specificity of the Pho13 enzyme.

From our metabolite profiling results, we observed higher abundances of free fatty acids (tetradecanoic, hexadecenoic, and octadecanoic acids) in *Sch. stipitis*. When it comes to the cofactor preference shift of XR in *Sch. stipitis*, XR shifts its redox cofactor preference to NADPH in the oxygen-available environment. High metabolic flux through NADPH-generating pathways is required to meet the demand on NADPH for xylose assimilation. Commonly, the oxidative pentose phosphate pathway is considered as a major route for generating NADPH, which functions as a driving force for the XR activity (Stincone et al. 2015; Kwak and Jin 2017; Jin et al. 2017). However, extra gluconeogenic anabolism is required to use the oxidative pentose phosphate pathway in Crabtree-negative strains like *Sch. stipitis*. To overcome this inefficient metabolic burden, we speculate that the cells could use mechanisms other than the oxidative pentose phosphate pathway for generating NADPH, e.g., enzymes such as cytosolic isocitrate dehydrogenase and malic enzyme associated with an increase in fatty acid synthesis and lipid accumulation (Koh et al. 2004; Zhang et al. 2007). Although it is unclear how *Sch. stipitis* splits NADPH into xylose assimilation and fatty acid synthesis, the mechanism for balancing $NADP^+$ and NADPH could be different from *S. cerevisiae* SR8.

In this study, we investigated the phenotypic and metabolomic differences between an innate xylose-utilizing yeast (*Sch. stipitis*) and an engineered xylose-utilizing yeast (*S. cerevisiae* SR8). The identified metabolic differences between *Sch. stipitis* and SR8 suggest efficient ways to control the redox balance in *Sch. stipitis*. We expect that these results will provide insights on how to control and balance redox cofactors for the production of fuels and chemicals from xylose by the engineered *S. cerevisiae*.

Compliance with ethical standards

Conflict of interest The authors declare that they have no conflicts of interest.

Ethical approval This article does not contain any studies with human participants or animals performed by any of the authors.

References

Acevedo A, Conejeros R, Aroca G (2017) Ethanol production improvement driven by genome-scale metabolic modeling and sensitivity analysis in *Scheffersomyces stipitis*. PLoS One 12:0180074. https://doi.org/10.1371/journal.pone.0180074

du Preez JC, Prior BA (1985) A quantitative screening of some xylose-fermenting yeast isolates. Biotechnol Lett 7:241–246. https://doi.org/10.1007/BF01042370

Hahn-Hägerdal B, Karhumaa K, Fonseca C, Spencer-Martins I, Gorwa-Grauslund MF (2007) Towards industrial pentose-fermenting yeast strains. Appl Microbiol Biotechnol 74:937–953. https://doi.org/10.1007/s00253-006-0827-2

Hilliard M, Damiani A, He QP, Jeffries T, Wang J (2018) Elucidating redox balance shift in *Scheffersomyces stipitis*' fermentative metabolism using a modified genome-scale metabolic model. Microb Cell Factories 17:140. https://doi.org/10.1186/s12934-018-0983-y

Ho NW, Chen Z, Brainard AP (1998) Genetically engineered *Saccharomyces* yeast capable of effective cofermentation of glucose and xylose. Appl Environ Microbiol 64:1852–1859

Hong K-K, Nielsen J (2012) Metabolic engineering of *Saccharomyces cerevisiae*: a key cell factory platform for future biorefineries. Cell Mol Life Sci 69:2671–2690. https://doi.org/10.1007/s00018-012-0945-1

Hou X (2012) Anaerobic xylose fermentation by *Spathaspora passalidarum*. Appl Microbiol Biotechnol 94:205–214. https://doi.org/10.1007/s00253-011-3694-4

Jeffries TW, Van Vleet JRH (2009) *Pichia stipitis* genomics, transcriptomics, and gene clusters. FEMS Yeast Res 9:793–807. https://doi.org/10.1111/j.1567-1364.2009.00525.x

Jin X-M, Chang Y-K, Lee JH, Hong S-K (2017) Effects of increased NADPH concentration by metabolic engineering of the pentose phosphate pathway on antibiotic production and sporulation in *Streptomyces lividans* TK24. J Microbiol Biotechnol 27:1867–1876. https://doi.org/10.4014/jmb.1707.07046

Jung YH, Kim S, Yang J, Seo J-H, Kim KH (2017) Intracellular metabolite profiling of *Saccharomyces cerevisiae* evolved under furfural. Microb Biotechnol 10:395–404. https://doi.org/10.1111/1751-7915.12465

Kim SR, Skerker JM, Kang W, Lesmana A, Wei N, Arkin AP, Jin Y-S (2013) Rational and evolutionary engineering approaches uncover a small set of genetic changes efficient for rapid xylose fermentation in *Saccharomyces cerevisiae*. PLoS One 8:57048. https://doi.org/10.1371/journal.pone.0057048

Kim SR, Xu H, Lesmana A, Kuzmanovic U, Au M, Florencia C, Oh EJ, Zhang G, Kim KH, Jin Y-S (2015) Deletion of PHO13, encoding haloacid dehalogenase type IIA phosphatase, results in upregulation of the pentose phosphate pathway in *Saccharomyces cerevisiae*. Appl Environ Microbiol 81:1601–1609. https://doi.org/10.1128/AEM.03474-14

Koh H-J, Lee S-M, Son B-G, Lee S-H, Ryoo ZY, Chang K-T, Park J-W, Park D-C, Song BJ, Veech RL, Song H, Huh T-L (2004) Cytosolic NADP+-dependent isocitrate dehydrogenase plays a key role in lipid metabolism. J Biol Chem 279(38):39968–39974. https://doi.org/10.1074/jbc.M402260200

Kötter P, Amore R, Hollenberg CP, Ciriacy M (1990) Isolation and characterization of the *Pichia stipitis* xylitol dehydrogenase gene, XYL2, and construction of a xylose-utilizing *Saccharomyces cerevisiae* transformant. Curr Genet 18:493–500

Kuznetsova E, Proudfoot M, Gonzalez CF, Brown G, Omelchenko MV, Borozan I, Carmel L, Wolf YI, Mori H, Savchenko AV, Arrowsmith CH, Koonin EV, Edwards AM, Yakunin AF (2006) Genome-wide analysis of substrate specificities of the *Escherichia coli* haloacid dehalogenase-like phosphatase family. J Biol Chem 281:36149–36161. https://doi.org/10.1074/jbc.M605449200

Kwak S, Jin Y-S (2017) Production of fuels and chemicals from xylose by engineered *Saccharomyces cerevisiae*: a review and perspective. Microb Cell Factories 16:82. https://doi.org/10.1186/s12934-017-0694-9

Lemus MR, Roussarie E, Hammad N, Mougeolle A, Ransac S, Issa R, Mazat J-P, Uribe-Carvajal S, Rigoulet M, Devin A (2018) The role of glycolysis-derived hexose phosphates in the induction of the Crabtree effect. J Biol Chem 293(33):12843–12854. https://doi.org/10.1074/jbc.RA118.003672

Øverland M, Skrede A (2017) Yeast derived from lignocellulosic biomass as a sustainable feed resource for use in aquaculture. J Sci Food Agric 97:733–742. https://doi.org/10.1002/jsfa.8007

Peeters K, Van Leemputte F, Fischer B, Bonini BM, Quezada H, Tsytlonok M, Haesen D, Vanthienen W, Bernardes N, Gonzalez-Blas CB, Janssens V, Tompa P, Versées W, Thevelein JM (2017) Fructose-1,6-bisphosphate couples glycolytic flux to activation of Ras. Nat Commun 8:922. https://doi.org/10.1038/s41467-017-01019-z

Rho HS, Choi K (2018) Cofactor regeneration using permeabilized *Escherichia coli* expressing NAD(P)+-dependent glycerol-3-phosphate dehydrogenase. J Microbiol Biotechnol 28:1346–1351. https://doi.org/10.4014/jmb.1803.03005

Silva JPA, Mussatto SI, Roberto IC (2010) The influence of initial xylose concentration, agitation, and aeration on ethanol production by *Pichia stipitis* from rice straw hemicellulosic hydrolysate. Appl Biochem Biotechnol 162:1306–1315. https://doi.org/10.1007/s12010-009-8867-6

Stincone A, Prigione A, Cramer T, Wamelink MMC, Campbell K, Cheung E, Olin-Sandoval V, Grüning N-M, Krüger A, Tauqeer Alam M, Keller MA, Breitenbach M, Brindle KM, Rabinowitz JD, Ralser M (2015) The return of metabolism: biochemistry and physiology of the pentose phosphate pathway. Biol Rev Camb Philos Soc 90:927–963. https://doi.org/10.1111/brv.12140

Tantirungkij M, Nakashima N, Seki T, Yoshida T (1993) Construction of xylose-assimilating *Saccharomyces cerevisiae*. J Ferment Bioeng 75:83–88. https://doi.org/10.1016/0922-338X(93)90214-S

Toivari MH, Aristidou A, Ruohonen L, Penttilä M (2001) Conversion of xylose to ethanol by recombinant *Saccharomyces cerevisiae*: importance of xylulokinase (XKS1) and oxygen availability. Metab Eng 3:236–249. https://doi.org/10.1006/mben.2000.0191

Veras HCT, Parachin NS, Almeida JRM (2017) Comparative assessment of fermentative capacity of different xylose-consuming yeasts. Microb Cell Factories 16:153. https://doi.org/10.1186/s12934-017-0766-x

Walfridsson M, Hallborn J, Penttilä M, Keränen S, Hahn-Hägerdal B (1995) Xylose-metabolizing *Saccharomyces cerevisiae* strains overexpressing the TKL1 and TAL1 genes encoding the pentose phosphate pathway enzymes transketolase and transaldolase. Appl Environ Microbiol 61:4184–4190

Zhang Y, Adams IP, Ratledge C (2007) Malic enzyme: the controlling activity for lipid production? Overexpression of malic enzyme in *Mucor circinelloides* leads to a 2.5-fold increase in lipid accumulation. Microbiology 153(7):2013–2025. https://doi.org/10.1099/mic.0.2006/002683-0

Zhang G-C, Liu J-J, Ding W-T (2012) Decreased xylitol formation during xylose fermentation in *Saccharomyces cerevisiae* due to overexpression of water-forming NADH oxidase. Appl Environ Microbiol 78(4):1081–1086. https://doi.org/10.1128/AEM.06635-11